

Supporting Information

Wang et al. 10.1073/pnas.1300233110

SI Materials and Methods

Cells and Virus. Human rhabdomyosarcoma (RD) cells, human THP-1 cells, and African green monkey Vero cells were cultured in DMEM (Invitrogen) supplemented with 10% (vol/vol) FBS at 37 °C in an incubator with 5% (vol/vol) CO₂. Human enterovirus type 71 (EV71) strain A12 was isolated from a patient with hand-foot-and-mouth disease and was identified as genotype C4. In vitro and in vivo characterization demonstrated A12 was non-virulent in suckling mice with ideal attenuated characteristics (1). The virus stock was prepared and titrated in RD cells, and it was stored at -70 °C until use.

Indirect Immunofluorescence Assay. RD cells at 80–90% confluence were infected with EV71, EV71-W6, or EV71-W6-calcium phosphate (CaP) at the desired multiplicity of infection (MOI), and 12–24 h postinfection, the infected cells were fixed with acetone at -20 °C for 30 min. The infected cells were then washed with PBS and incubated with mice antisera against EV71 or calcium chelating agent W6p peptide for 1 h, followed by three washes with PBS, and they were then incubated with Alexa Fluor 488-conjugated goat anti-mouse IgG as the secondary antibody for 30 min. The fluorescence was detected after washing with PBS. DAPI was added, and the cells were incubated at room temperature for 5 min to stain the nuclei.

Plaque Assays. Ninety percent confluent RD cells in a 12-well plate were infected with 400 µL of serial 10-fold viral dilutions. After 1 h of adsorption, the infected cells were washed and incubated for 3 d with DMEM containing 2% (vol/vol) FBS and 1% (wt/vol) low-melting-point agarose. The cells were fixed with 4% formaldehyde and stained with crystal violet solution [1% (wt/vol) crystal violet, 0.85% (wt/vol) NaCl, 2% (wt/vol) formaldehyde].

One-Step Growth Curves. Viral growth curves in RD and Vero cells were determined in a 24-well plate with parental EV71, EV71-W6, and EV71-W6-CaP, respectively, at the desired MOI. The supernatants were collected at intervals, and the titers were examined by plaque assays as previously described.

EM Characterizations. The viral solutions were added onto carbon-coated copper transmission electron microscopy (TEM) grids (400 mesh; Agar Scientific) by dip-coating, and the samples were then dried at room temperature before observation. The samples were also stained with phosphotungstic acid. TEM observations were performed using a JEM-1200EX microscope (JEOL). SEM and energy dispersive X-ray spectroscopy analyses were performed using a JSM-35CF microscope (JEOL). Samples were prepared by dispersing 50 µL of solution on the surface of silica specimen stubs. They were dried at 30 °C for at least 24 h and were sputter-coated with gold before the examinations.

Thermal Stability Tests. EV71-W6-CaP, EV71-W6, and parental EV71 were incubated at 26 °C, 37 °C, and 42 °C, respectively, and samples were collected periodically. The remaining infectivity was determined by plaque assays as previously described (2).

One-Step Quantitative Real-Time RT-PCR Method. Viral RNA was extracted using an RNA Purelink RNA mini kit (Ambion) following the manufacturer's instructions. The obtained RNA was quantified by one-step quantitative real-time RT-PCR using a One Step PrimeScript RT-PCR Kit (Takara) according to the manufacturer's instructions with EV71-specific forward primer

(5'-GGCCATTTATGTGGGTAACITTTAGA-3'), reverse primer (5'-CGGGCAATCGTGTCAACAAC-3'), and probe (5'-FAM-AAGACAGCTCTCGCGACTTGCTCGTG-BQH1-3'). Absolute quantification of RNA was calculated according to the standard curve, which was generated by serially diluting an RNA solution of determined titer in sterile water.

Dot Plot Assays. For immunological detection of EV71 coat proteins, 10⁶ plaque-forming units each of bare EV71-W6 and EV71-W6-CaP were spotted onto a 100% methane-activated PVDF membrane (Millipore) and the membrane was then air-dried at room temperature. Nonspecific binding sites were blocked using 5% skim milk in PBS. The membrane was then probed with a polyclonal antibody specific to EV71, followed by an alkaline phosphatase-conjugated horse anti-mouse antibody. Both antibodies were diluted in blocking solution (0.05% BSA). Signals were generated by the addition of 5-bromo-4-chloro-3-isidolyl phosphate/nitro blue tetrazolium (BCIP/NBT).

Neurovirulence Tests. The neurovirulence of EV71, EV71-W6, and EV71-W6-CaP was examined as previously described (3). Briefly, the rescued virus was diluted and then intracranially inoculated into the 3-d-old BALB/c suckling mice (*n* = 5 per group). All mice were monitored daily for clinical symptoms and death until 14 d after inoculation.

ELISA. Detection of serum IgG antibodies against EV71 was performed by indirect ELISA using 96-well, flat-bottomed plates (Costar) coated with EV71 control strain A12 diluted 1:100 in 0.1 M carbonate/bicarbonate buffer (pH 9.6) overnight at 4 °C. After blocking with 5% skim milk powder in PBS and Tween 20 (PBST), plates were incubated with serially diluted sera in duplicate wells for 1 h at 37 °C. Peroxidase-conjugated horse anti-mouse IgG at a dilution of 1:5,000 was then added and incubated for 0.5 h at 37 °C, followed by the substrate BCIP/NBT. Plates were washed with PBST (pH 7.2) three times with an interval of 5 min after each reaction. Absorbance of the color developed was determined at 492 nm and corrected for background with PBS control group sera.

Microneutralization Assays. Mice serum was serially twofold diluted in DMEM starting at a ratio of 1:8. A 50-µL virus suspension at 100-fold the 50% tissue culture infective dose was mixed with 50 µL of sera, and the mixtures were incubated at 37 °C for 1 h. The mixtures were then added to 60% confluent Vero cells and incubated for 7 d. Appropriate serum, virus, and cell control was included in the test. The end-point titers were calculated using the Reed–Muench method (4) as previously described (5).

IFN-γ Enzyme-Linked Immunospot Assays. IFN-γ enzyme-linked immunospot assays of a mouse set (BD Biosciences) were performed according to the manufacturer's instructions (6, 7). Briefly, 96-well filtration plates were coated overnight at 4 °C with IFN-capture monoclonal antibody, followed by washing and blocking with RPMI-1640 medium containing 1% L-glutamine and 10% FBS for 2 h at room temperature. Splenocytes (5 × 10⁵ cells per well) were then added in RPMI-1640, with the subsequent addition of native EV71 as the stimulation antigen, and cultured for 20 h at 37 °C under 5% CO₂. After washing with water once and washing with PBST three times, plates were incubated with biotinylated IFN-γ detection antibody at room temperature for 2 h, followed by three washes with PBST and 1 h

of incubation with streptavidin HRP at room temperature. Spots were revealed using an AEC substrate reagent set (BD Bioscience) at room temperature and were counted with an Immunospot reader (Cellular Technology).

Statistical Analysis. The statistical significance of differences in antibody titers among different groups was determined by the paired Student *t* test using SPSS software (IBM). Results with error bars are expressed as the SDs.

1. Chang GH, et al. (2010) Sequence analysis of six enterovirus 71 strains with different virulences in humans. *Virus Res* 151(1):66–73.
2. Wiggan O, et al. (2011) Novel formulations enhance the thermal stability of live-attenuated flavivirus vaccines. *Vaccine* 29(43):7456–7462.
3. Han JF, et al. (2010) Producing infectious enterovirus type 71 in a rapid strategy. *Virol J* 7:116.
4. Reed L, Muench H (1938) A simple method of estimating fifty per cent endpoints. *Am J Epidemiol* 27(3):493–497.
5. Chang LY, et al. (2004) Transmission and clinical features of enterovirus 71 infections in household contacts in Taiwan. *JAMA* 291(2):222–227.
6. Costa SM, et al. (2011) Induction of a protective response in mice by the dengue virus NS3 protein using DNA vaccines. *PLoS ONE* 6(10):e25685.
7. Yauch LE, et al. (2009) A protective role for dengue virus-specific CD8+ T cells. *J Immunol* 182(8):4865–4873.

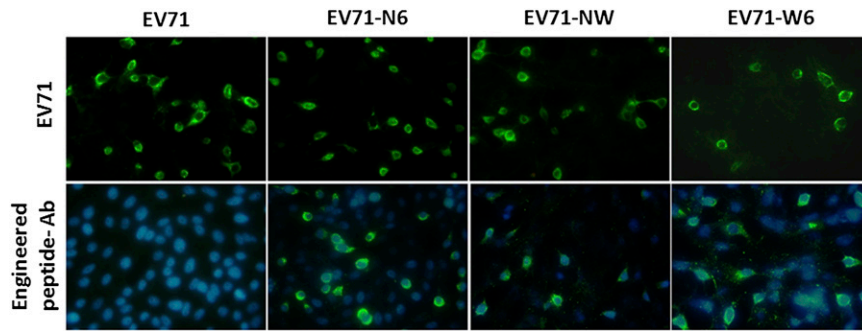


Fig. S1. Indirect immunological fluorescence of parental EV71 and recovered engineered viruses on Vero cells with EV71-specific polyantibody (*Upper*) or with nucleating peptide-specific polyantibodies (*Lower*). The green fluorescence indicates the successful expression of engineered peptides on the viral surface, and the blue fluorescence represents the nucleus stained by DAPI. (Magnification: 40 \times .)

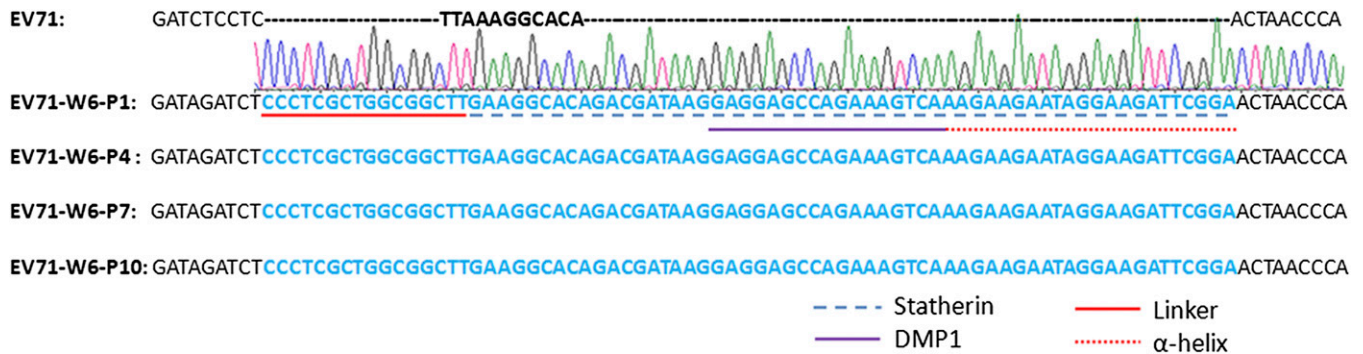


Fig. S2. Genetic stability of the engineered peptide's coding sequence. After 10 generations, the viral RNA of passage 1, 4, 7, and 10 progeny viruses was extracted and sequenced, and the results showed that it was relatively stable.

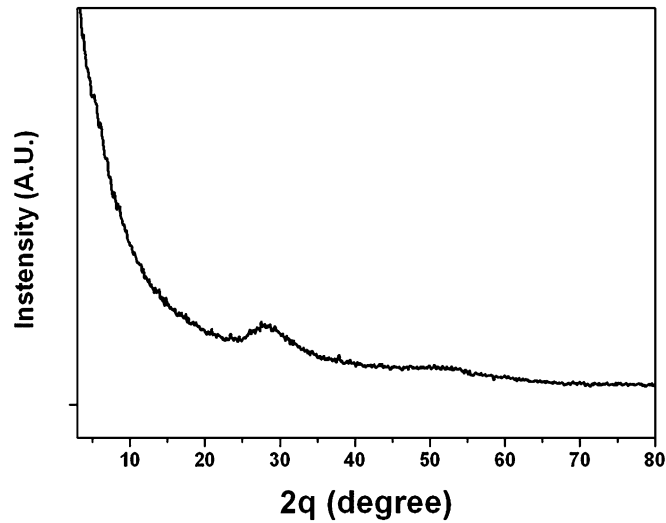


Fig. S3. X-ray diffraction analysis of self-biomineralized viral particles. The pattern indicated the formation of a CaP mineral phase around the vaccine was amorphous. A.U., arbitrary unit; 2q, two theta.

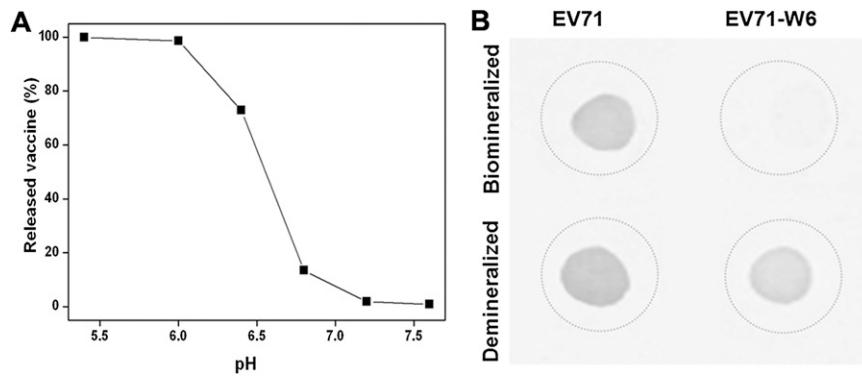


Fig. S4. (A) pH-sensitive release of enclosed EV71-W6 from EV71-W6-CaP particles. A total of 10^7 plaque-forming units of EV71-W6-CaP in DMEM were collected, diluted in Tris-buffered saline (TBS) solution of different pH, and incubated for 0.5 h. The amount of released vaccine was estimated by quantifying the viral RNA in the supernatant by the quantitative RT-PCR method after centrifugation ($16,000 \times g$ for 10 min); square represents percentage of released EV71-W6 vaccines at indicated pH. (B) Dot-blotting assays of biomineralized or demineralized EV71 and EV71-W6. At physiological pH 7.4, the CaP biomineralized exterior was rather stable and viral antigens could not be detected by EV71-specific antibodies, whereas the CaP exterior was demineralized at pH less than 6.5 and the viral antigens were detectable again.

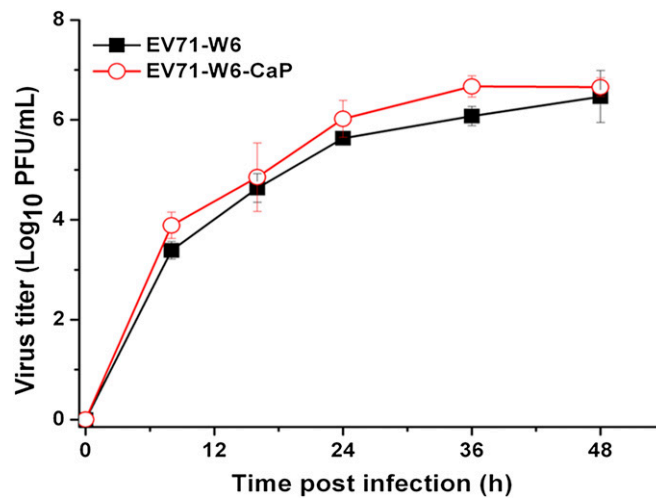


Fig. 55. One-step growth curves of EV71-W6-CaP or bare EV71-W6 on RD cells at MOI = 0.1 ($n \geq 3$); error bars represent SDs.

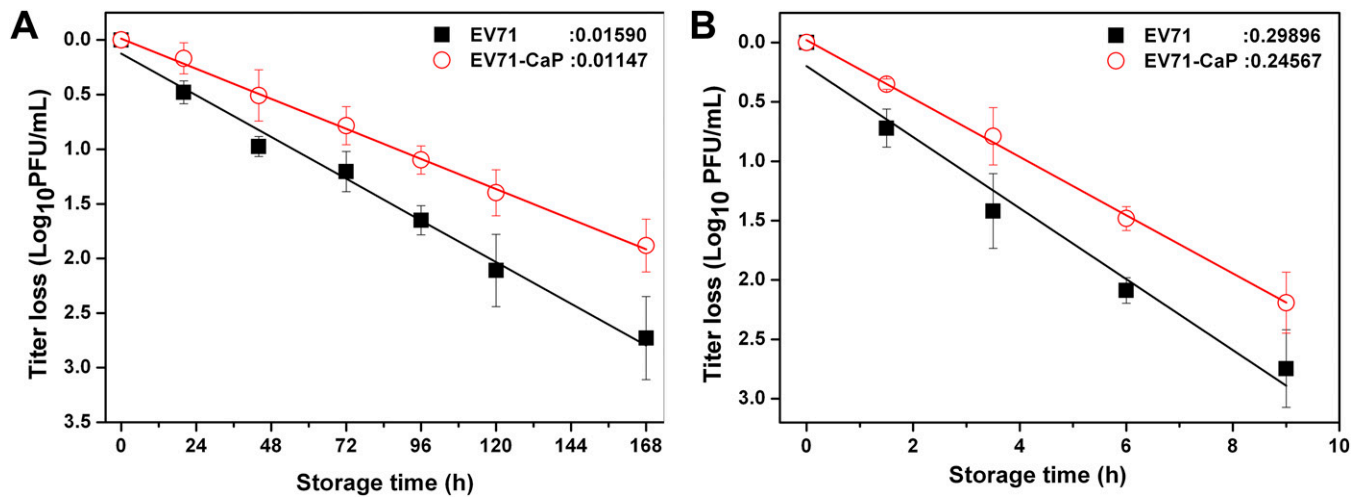


Fig. 56. In vitro test of virus thermostability. Thermal-inactivation kinetics were determined at 37°C (A) or 42°C (B). The remaining percentage of infectivity was represented in a logarithmic scale as a function of storage time ($n \geq 3$); error bars represent SDs. The calculated average inactivation rate constants for EV71 and EV71-CaP, as shown in the figure, were $K_{EV71} = 0.0159 \text{ h}^{-1}$ and $K_{EV71-CaP} = 0.01147 \text{ h}^{-1}$ at 37°C and $K_{EV71} = 0.29896 \text{ h}^{-1}$ and $K_{EV71-CaP} = 0.24567 \text{ h}^{-1}$ at 42°C.

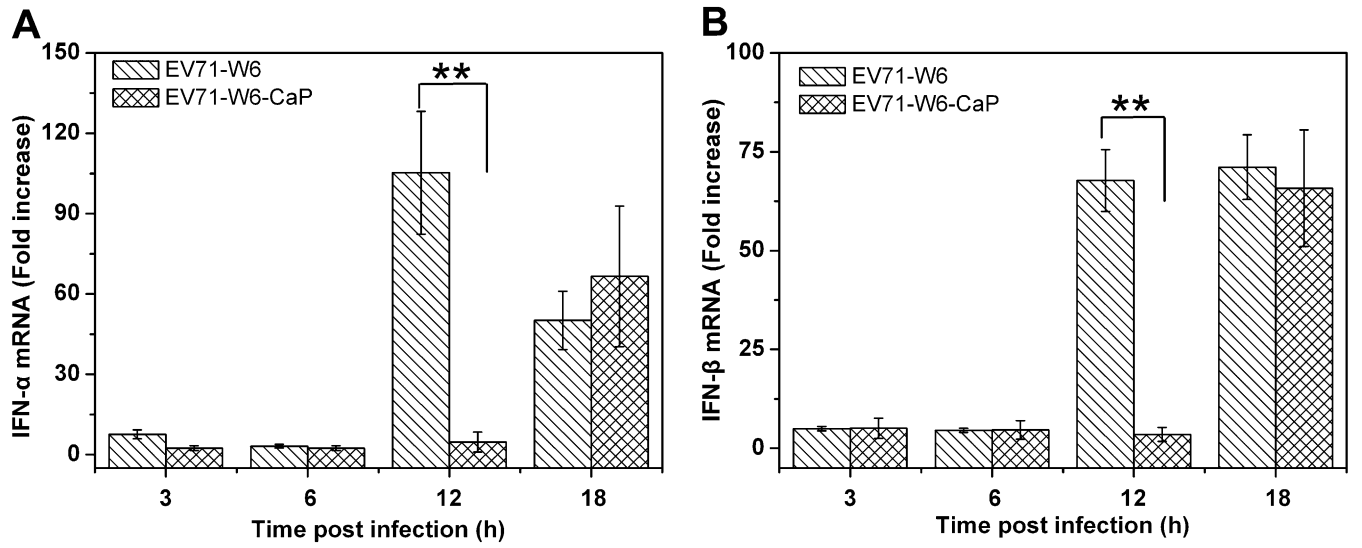


Fig. S7. Expression levels of IFN- α (A) and IFN- β (B) on RD cells activated by EV71-W6 and EV71-W6-CaP were measured by quantitative RT-PCR at intervals postinfection; error bars represent SDs ($n \geq 3$, Student's paired t test, one-tailed, $**P < 0.01$).